Appl. Phys. B 85, 611–617 (2006)
DOI: 10.1007/s00340-006-2268-0

Applied Physics B
Lasers and Optics

A. GAMUCCI[1,2,3,✉]
M. GALIMBERTI[1,3]
D. GIULIETTI[1,2,3]
L.A. GIZZI[1,3]
L. LABATE[1,4]
C. PETCU[1,5]
P. TOMASSINI[1,3]
A. GIULIETTI[1,3]

Production of hollow cylindrical plasmas for laser guiding in acceleration experiments

[1] Intense Laser Irradiation Laboratory, IPCF, Consiglio Nazionale delle Ricerche, Area della Ricerca di Pisa, Via Moruzzi 1, 56124 Pisa, Italy
[2] Dipartimento di Fisica, Università di Pisa, Italy
[3] INFN, Sezione di Pisa, Italy
[4] Laboratori Nazionali di Frascati, INFN, Roma, Italy
[5] National Institute for Lasers, Plasma and Radiation Physics, Bucharest, Romania

Received: 13 March 2006/Revised version: 13 April 2006
Published online: 31 May 2006 •

ABSTRACT One of the major tasks for the progress of laser acceleration of electrons in plasmas is the guiding of focused pulses along path lengths much larger than the depth of focus. We have tested experimentally the production of hollow plasmas in gas to be used as guiding medium. We induced optical breakdown in Helium with a nanosecond laser pulse similar to the Amplified Spontaneous Emission (ASE) pedestal of a powerful ultrashort laser pulse. The plasma produced in this way was carefully characterized by high resolution interferometry. Plasma channels several millimeters in length whose density, depth and width match the requirements for an efficient guiding have been obtained. Channels with a variety of parameters can be created according to the well-known dynamics of the plasmas produced by optical breakdown.

PACS 42.82.Et; 52.50.Jm; 41.75.Jv

1 Introduction

The importance of stable and reproducible plasma channels is raising with the need of guiding high intensity laser pulses for various purposes. In this paper we report on the production of plasma channels that fit the requirements for laser wakefield acceleration (LWFA) experiments. In the LWFA scheme the laser pulse duration is related to the plasma wavelength and therefore to the plasma density [1] according to $c\tau \approx \lambda_{pe}/2$, where c is the speed of light, τ is the laser pulse duration and λ_{pe} is the wavelength of the electron plasma wave. By using this acceleration mechanism, recent experiments have demonstrated the production of hundreds of MeV electrons with acceleration lengths of hundreds of microns [2–5]. Among the experimental problems that have to be overcome in order to increase the electron energy reachable by exploiting this acceleration technique, one of the major tasks is the extension of the acceleration length. The aim is to go well beyond the optical limit given by the so called Rayleigh length. The general idea is based on the use of guiding techniques balancing the diffraction of the pulse [6–8]. One method for creating such optical guides relies on the use of gas-filled capillary or Z-pinch discharges [9, 10]. Another possibility is to create a channel with a precursor laser pulse, prior to the arrival of the main accelerating pulse [11]. This latter method has been recently improved by using clustered gas-jets and generating the plasma waveguide with an ultrashort precursor pulse (70 fs). In this way the propagation of a femtosecond test pulse through the plasma waveguide was successfully proved [12]. The method based on clustered gases has been then extended to longer pulses (100 ps) with high efficiency allowed by the high laser pulse absorption compared with the unclustered case [13]. Though experiments with clustered gases are of great interest, our work shows that also the simple gas breakdown obtained with pulses similar to the ASE precursor of a powerful femtosecond pulse can produce suitable guiding conditions, as we will discuss below. Here we just recall that a relation has been established between the depth and the radius of a parabolic plasma channel and the laser spot size for a gaussian pulse to obtain the best guiding effect [7]. It has also been recently proved [14] that tapered plasma channels, in which the electron density on the longitudinal axis raises along the coordinate of the pulse propagation, allow acceleration up to GeV energies to be obtained. We have produced plasma channels that basically fulfill all these requirements. Moreover, the plasmas were obtained with laser pulses similar to the nanosecond ASE (Amplified Spontaneous Emission) that typically precedes ultrashort powerful laser pulses produced with the Chirped Pulse Amplification (CPA) technique. This allows one to design experiments in which the ASE, usually a perturbation to the main interaction, can be turned into a useful tool to improve the conditions for acceleration. This kind of approach has been already successfully used in acceleration experiments using thin foils: in that case the ASE was used to explode the foil and to obtain a plasma of a suitable density [15].

2 The method

Laser pulses employed in acceleration experiments have typical durations of tens of femtoseconds, but a nanosecond pedestal precedes the short pulse due to ASE, whose intensity is several orders of magnitude lower than the high intensity one. Usually, laser pulses employed for acceleration purposes have a peak intensity on target exceeding 10^{+19} W/cm^2, while the ratio to the ASE intensity is typic-

✉ Fax: +39-050 3152230, E-mail: andrea.gamucci@ipcf.cnr.it

ally of the order of 10^6. On the other hand, an ASE pre-pulse intensity of 10^{13} W/cm^2 is by far above the threshold for gas breakdown, so that the short femtosecond pulse usually propagates in a pre-formed plasma rather than in a gas.

Our aim was to find the most suitable conditions to improve the acceleration length. To this purpose we used the well-established data [16] on optical gas breakdown by laser pulses and subsequent evolution of the plasma. Basically, a small plasma is initially produced by optical breakdown in the gas nearby the focus; then the plasma expands along the laser propagation axis due to the fastest of the following two phenomena: (i) the "propagation" of the condition for the optical breakdown at the leading edge of the laser pulse, or (ii) the propagation of the blast wave produced by the local fast heating of the gas. Whatever the mechanism, if the initial plasma is optically thick to the laser radiation (heavy gases and/or high pressure) the plasma will expand only toward the laser. In the opposite case of optically thin plasmas, expansion will take place in both directions, producing a quasi cylindrical region of ionized gas, nearly symmetric with respect to the focal position.

In our experiment, as well as in most of acceleration experiments with gas targets, optically thin and then symmetric plasmas are produced. The use of large f/N number, particularly suitable for acceleration, enables the nanosecond pulse to produce a plasma whose length on the laser propagation axis is much larger than the transverse size. Further, in the nanosecond time-scale, the transverse expansion of the hot plasma in the surrounding gas will result in a density depletion along the axis, as expected from a quasi cylindrical explosion. We show that in this way, it is possible to create plasmas able to support long-scale acceleration for high gain acceleration experiments.

3 The experiment: set-up and data analysis

The experiment described here was performed at the ILIL Laboratory, in collaboration with the SLIC Laboratory of CEA in Saclay (France). The laser used for the experiment is a two beams 3 GW Neodymium laser (YLF oscillator, phosphate glass amplifiers), wavelength $\lambda = 1053$ nm, pulses of 3 ns FWHM. The laser operates in single longitudinal mode. The system can provide intensities up to 10^{15} W/cm^2 on target with a high temporal and spatial quality. One of the beams (called "main") was used to produce the plasma and the other (called "probe") was devoted to the interferometry. The main beam was focused in a spot of ~ 12 μm diameter by a $f/8$ lens in a Helium gas-jet. We chose a particular range of energies: from 0.3 J to 0.5 J per pulse to be close to the intensity of a typical ASE pre-pulse.

The expertise of the CEA laboratories on the gas-jet production and characterization [17] was a basic contribution to this work.

The gas-jet nozzle we have used in this case was a rectangular slit of 3 mm × 0.3 mm and the gas-jet had already been characterized [18]. The laser beam axis was set to be in the longitudinal symmetry plane of the gas-jet. Data were taken focusing the beam at different distances from the entrance to the exit of the gas-jet. The geometry of the focusing conditions is shown in Fig. 1.

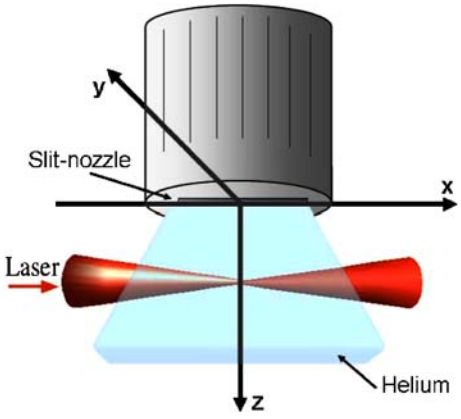

FIGURE 1 Gas-jet and laser focusing geometry. The coordinate system used in the text is shown. The focus of the beam was moved from the center (as shown here) towards either the entrance or the exit in the gas-jet. The probe beam, not shown in Figure, is directed along the y axis

In this paper we consider, in particular, three different positions of the focus: $x = 0$ (focal spot in the center of the nozzle), $x = \pm 1$ mm. The laser beam axis was 500 μm away from the nozzle plane.

The probe beam was frequency doubled using a KDP crystal and delayed with respect to the main beam. A Nomarski interferometer [19, 20] was used for observing interferometric images of the plasma; the fringes were recorded on a CCD camera. As it is well known, the Nomarski interferometer employs two polarizers, a lens and a Wollaston prism: one of the polarizers is set before the prism and the other one after it, allowing the two orthogonally polarized images of the plasma to interfere and give a fringe pattern. The interferometer was designed and set up in order to have high fringe visibility and a spatial resolution well below 10 μm. By changing the path of the probe beam by means of a sliding prism to set the delay with respect to the main beam, it was possible to study the plasma evolution. However in this paper we only consider interferograms obtained with a delay of 5 ns.

The phase map was deconvoluted using a fringe analysis technique based on Continuous Wavelet Transform Ridge Extraction [21], thus obtaining the phase-shift distribution in the $x - z$ plane with a high degree of accuracy. In particular, this technique is able to evidence local variations of phase better than other techniques based on Fast Fourier Transforms. The phase difference maps were in turn processed with an improved Abel inversion algorithm [22] in which the usual axial symmetry requirement is relaxed by means of a truncated Legendre polynomial expansion in the azimuthal angle. With this procedure we obtained, from the three interferograms in Fig. 2, the data on the electron density shown in Fig. 3 to Fig. 5, next section.

4 The experimental data

A large number of interferograms were obtained with the set-up described in the previous section. Many experimental parameters were varied in order to investigate different regimes. The most interesting for LWFA was found when the laser beam was 500 μm away from the nozzle. In this region of the gas-jet the Helium density, as derived from

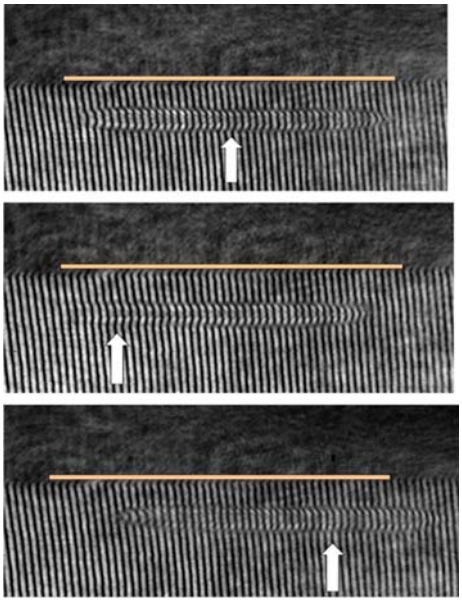

FIGURE 2 Fringe patterns for the plasma obtained focusing the main pulse at $y = 0$, $z = 500\,\mu$m. Top: $x = 0$, energy 460 mJ; middle: $x = -1$ mm, energy 460 mJ; bottom: $x = +1$ mm, energy 490 mJ. The *arrow* indicates the focus position and the horizontal line indicates the 3 mm gas-jet slit position. The laser propagates from the left

the measurement of the electron density, is of the order of $5 \times 10^{18}\,\mathrm{cm}^{-3}$.

The interferograms showed high shot-to-shot reproducibility of the plasmas. Figure 2 shows three typical interferograms obtained focusing the main beam in the three positions, namely $x = 0$, $x = \pm 1$ mm. Energy ranged from 460 mJ to 490 mJ.

According to these figures, the plasma basically has cylindrical structure regardless of the position of the focus, as it is clear from the patterns shown in Fig. 2. The Figure refers to shots performed focusing the main pulse respectively at $x = 0$ (top), $x = -1$ mm (middle), $x = +1$ mm (bottom), while in all the three cases was $y = 0$, $z = 500\,\mu$m.

The plasma length was found to be about 3 mm. It is shorter than the full available gas length which is of about 4 mm (at half of the maximum density) at 500 μm from the slit.

5 Discussion

The three interferograms shown in the previous Section are representative of a large number of data characterized by a high reproducibility. From their analysis we see that in conditions of interest for laser acceleration of electrons in Helium (with suitable density, f/N, intensity and pulse duration) one can obtain quasi-cylindrical plasmas of several millimeters length with a hollow channel on their axis. From previous data [23] we know that the electron temperature of our plasma is $T_e \approx 50$ eV. At the density of our plasma, this implies a complete ionization of the He gas in the plasma volume [24]. In the following, we will mostly refer to the electron density n_e as simply "density".

From the analysis of the interferograms we see that the plasma density on the axis of the channel ranges from 3.5 to

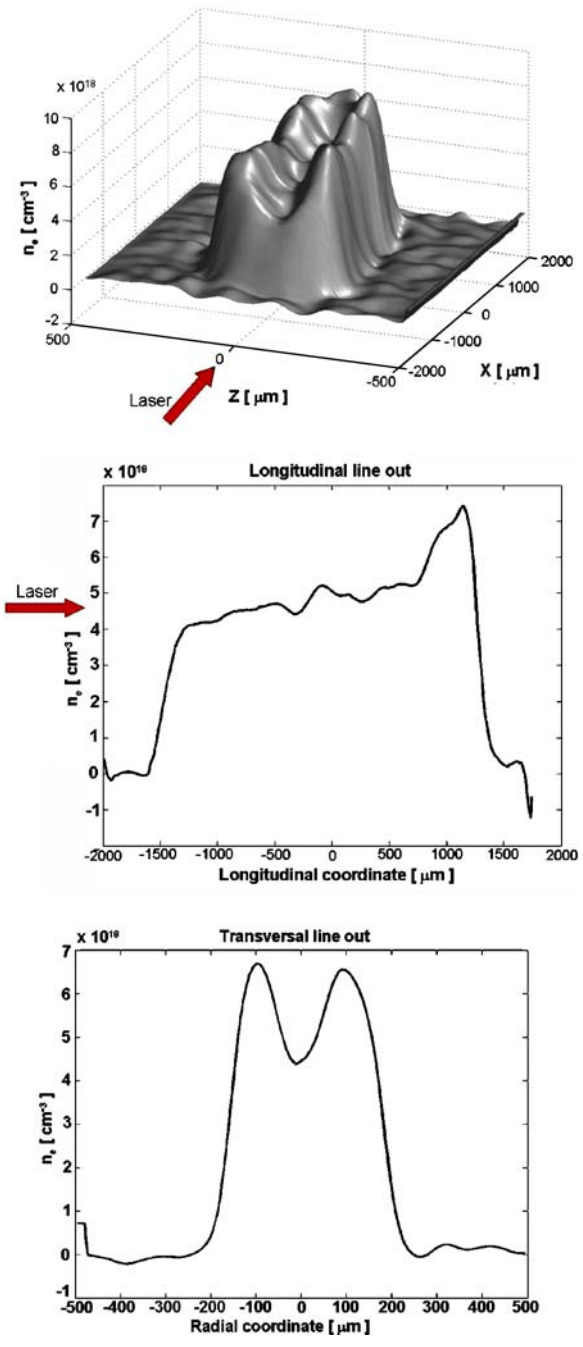

FIGURE 3 Electron density from the interferogram of Fig. 2 (*top*). *Top*: 3D reconstruction of the plasma density distribution. *Middle*: density line out on the longitudinal axis. *Bottom*: transversal density line out taken at $x \approx -300\,\mu$m. The origin of the z axis corresponds to 500 μm from the nozzle

$4.5 \times 10^{18}\,\mathrm{cm}^{-3}$. This is a range of density suitable for wakefield acceleration of electrons in plasmas with powerful laser pulses of few tens of femtoseconds. This value can be easily modified by properly choosing the initial density of the background gas.

The longitudinal density profile on the axis taken from interferograms 5 ns after the pulse peak, shows rising or falling of the density along the laser path. The density slope depends in sign and value upon the position of the focus with respect to the entrance border of the gas-jet. This fact can al-

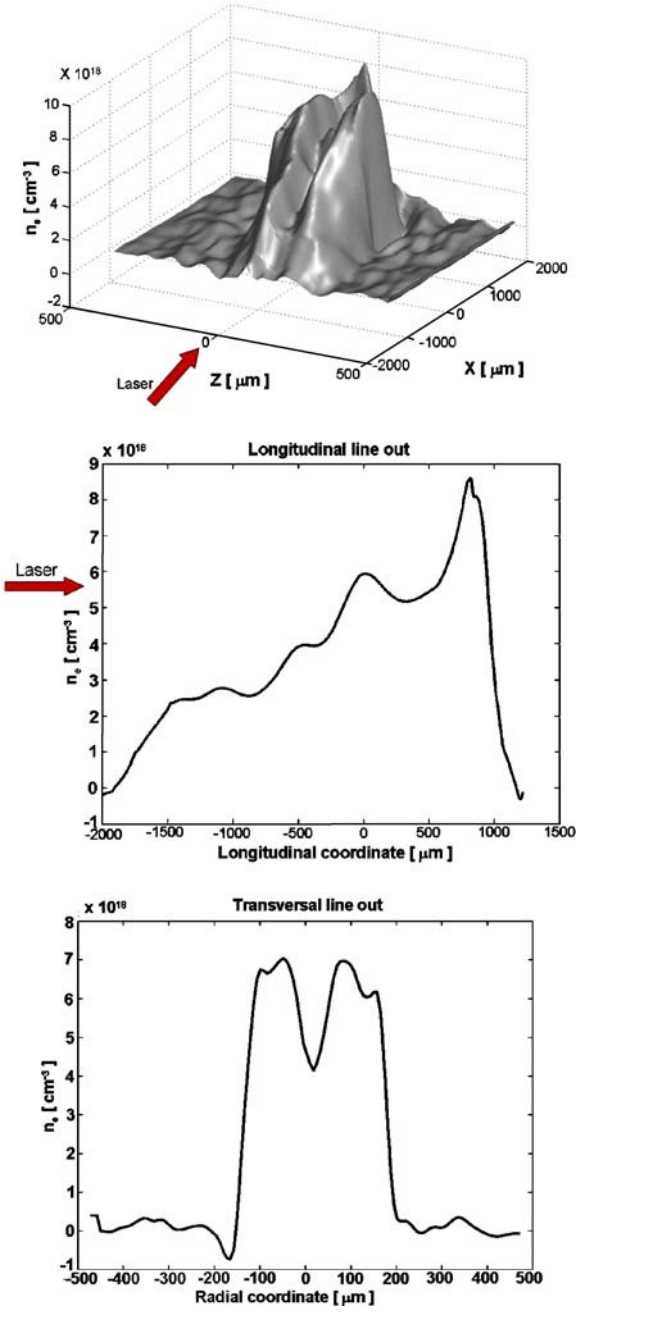

FIGURE 4 Electron density from the interferogram of Fig. 2 (*middle*). *Top*: 3D reconstruction of the plasma density distribution. *Middle*: density line out on the longitudinal axis. *Bottom*: transversal density line out taken at $x \approx -300\,\mu$m. The origin of the z axis corresponds to 500 μm from the nozzle

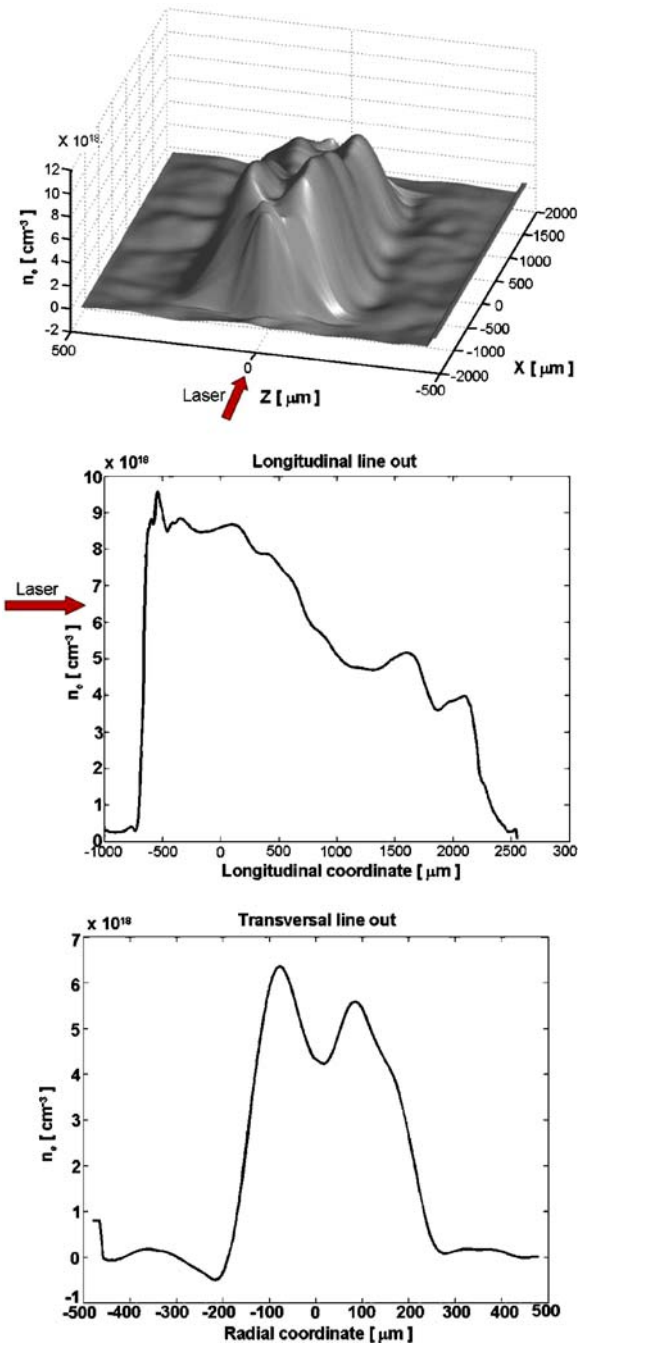

FIGURE 5 Electron density from the interferogram of Fig. 2 (*bottom*). *Top*: 3D reconstruction of the plasma density distribution. *Middle*: density line out on the longitudinal axis. *Bottom*: transversal density line out taken at $x \approx -100\,\mu$m. The origin of the z axis corresponds to 500 μm from the nozzle

low one to test different models and simulations on guiding and acceleration in plasma channels. As introduced above, acceleration in "tapered" channels has recently been considered and successfully simulated [14]. In Figs. 3 and 4 we see two different slopes of increasing density. The slope can be tuned by moving the focal position in the gas-jet. In all the cases, the maximum density along the plasma axis is 10^{19} cm^{-3} and is located at one end of the channel forming a "channel tip" of few tens of micrometers width. Density and depth of such a tip are the same of those of the cylindrical "wall" of the channel, as can be seen from the transverse density profiles in Fig. 3 to Fig. 5. In fact, both channel tips and walls are fronts of the detonation wave produced by the hot plasma in the cold surrounding gas. This is also consistent with the sharp gradient of the electron density at the external boundary of the plasma, with a scale length of 10 to 15 μm. It is worth noting that in all the three cases considered (Fig. 3 to Fig. 5) there is only one tip for each channel (either at the entrance or at the exit). This is because the other channel end is located in the region of lower density at the boundary of the gas-jet. A consequence of the latter observation is that chan-

nels with no tip at all can be produced with a larger f/N focusing, so that both channel ends fall outside the gas-jet boundaries. The transverse density profiles show a minimum whose value ranges from 60% to 70% of the maximum electron density at the channel wall. The radius of the channel at half of his depth ranges from 30 to 50 μm. These channel parameters are suitable for an efficient guiding of the accelerating laser pulse over paths much longer than the focal depth of the focused pulse.

As from the theory of optical guides, if the plasma refraction index peaks on its longitudinal axis, the portion of light wave front located nearby the axis of propagation can be retarded with respect to the peripheral part, thus allowing the beam to remain focused over many Rayleigh lengths. To further develop this point in our case let us notice that the channels we have produced show a basically parabolic transverse density profile.

In fact, Fig. 6 shows the magnification of the central region of the transversal line out in Fig. 3, with the parabolic curve that fits the experimental data. The electron density can be then described as $n_e(r) = n_0 + \Delta n_e (r/r_{ch})^2$, where the values n_0 and $\Delta n_e / r_{ch}^2$ resulting from the fit are: $n_0 = 4.542 \times 10^{18}\,\mathrm{cm}^{-3}$ and $\Delta n_e / r_{ch}^2 = 3.74 \times 10^{22}\,\mathrm{cm}^{-5}$. From this last fit parameter, we can estimate the radial parameter of the plasma channel, r_{ch}, taking Δn_e from the experimental electron density distribution, and we find $r_{ch} \approx 73$ μm. Moreover, we can find out the basic guiding properties of such a plasma channel, as whether there is a frequency cutoff or computing the high-order gaussian beam modes that can be supported by this quadratic index profile.

To evaluate these characteristics, we can substitute in the plasma index of refraction dependence on the electron density profile $\eta^2(r) = 1 - 4\pi n_e(r) e^2/m\omega^2$ the relation for $n_e(r)$ given above. Then, solving the vector-wave equation for the electric field from the Maxwell equations in a lens like medium [25], the "spot size" w_0 results to be $w_0 = [r_{ch}^2/(\pi \cdot r_e \Delta n_e)]^{0.25}$ where r_e is the classical electron radius. In our case $w_0 \approx 23$ μm. Pulses of smaller spot sizes can be guided with channels as the one of Fig. 4. It is worth noticing that from this last relation follows that the spot size that can be supported by a plasma guide like the one we considered does not depend on the frequency of the incoming radiation. We can thus infer that there is not a cutoff that binds the propagation of laser radiation in such a channel.

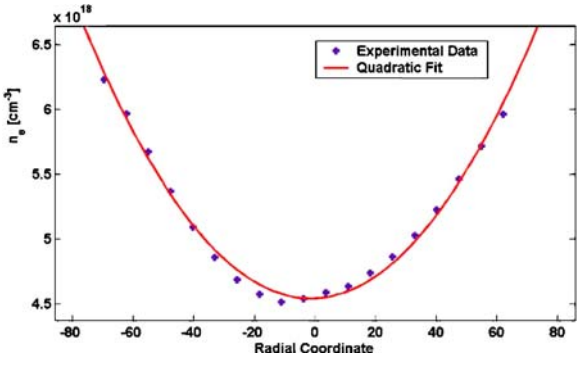

FIGURE 6 Magnification of the central part of the electron density line out of Fig. 3 (*bottom*), compared with the quadratic fit

Going further, one can now consider the analysis of the mode properties of these plasma waveguides, referring to three different models that describe the guiding conditions depending on the dimension of the channel [26]. Assuming that the n-order mode spot size evolves as $\sqrt{2p+|m|+1}$ times w_0, where $p \geq 0$ and m are radial and azimuthal mode indices and w_0 is the spot size found above (corresponding to the $1/e$ field radius of the $p = 0$, $m = 0$ mode), one sees that the constraint on the number of guided modes arises from the inequality $w_0\sqrt{2p+|m|+1} \leq r_{ch}$. We find that $2p + |m| + 1 \leq 10$, accounting for 55 modes capable to propagate in the plasma channel. In summary, the plasma channels that we obtained 5 ns after the nanosecond pulse peak can guide ultrashort pulses focused in spots of few tens of microns. This is an interesting scenario for acceleration.

A relevant point here is the reliability of the design of a plasma channel of suitable parameters for a given experiment. To discuss this point we use the well-established results on the production and evolution of plasmas in gases by laser-induced optical breakdown [16]. Figure 7 shows the basic features of the longitudinal expansion of a plasma produced by laser induced gas breakdown.

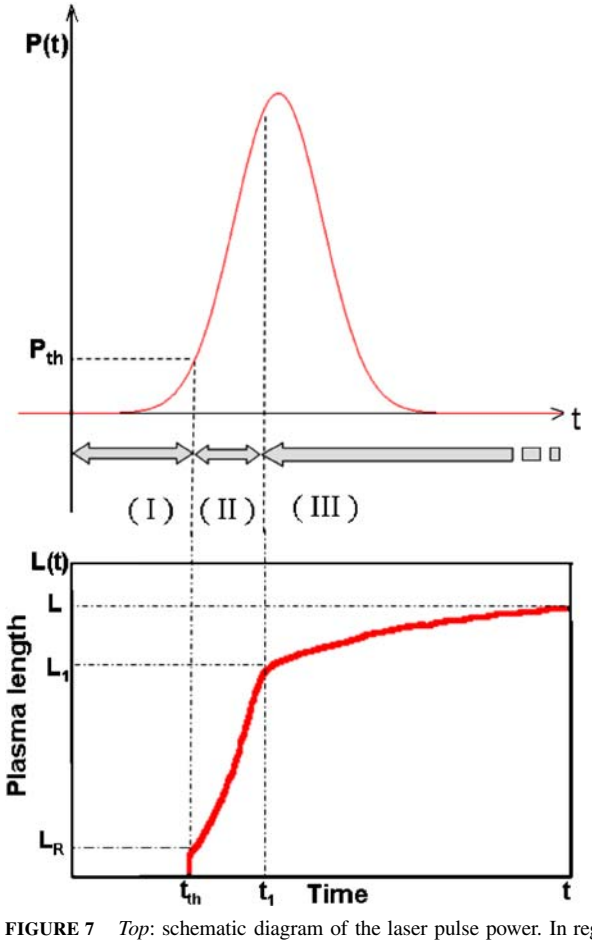

FIGURE 7 *Top*: schematic diagram of the laser pulse power. In region (I) the power is below the breakdown threshold value. In region (II) the main process responsible for the longitudinal plasma expansion is the "propagation" of the breakdown threshold condition. Finally – region (III) – the longitudinal plasma expansion is driven by the blast wave. *Bottom*: the plasma length versus time as derived from the model described in the text

The top diagram shows the power versus time $P(t)$ of a Gaussian laser pulse, as in our case. At the time t_{th} the laser pulse reaches the power P_{th} corresponding to the threshold intensity I_{th} at which breakdown occurs in the focal region. The gas ionizes in a very short time in a region whose length is comparable with the Rayleigh length L_R. The layer in the gas where the threshold condition is satisfied will shift progressively along the path of the beam, driven by the rise of the laser pulse intensity in the given geometry of the focusing optics (we are operating with a large f/N). Then, the longitudinal ionization front will follow the motion of this layer. This kind of fast propagation will continue until, at the time t_1, its velocity will decrease below the velocity of the blast wave. At the time t_1, before the pulse peak, the plasma length is L_1. The longitudinal plasma expansion is now driven by a blast wave supported by the laser energy deposition. Finally, the later stage of the plasma expansion will be driven by a blast wave whose velocity decreases in time. In our experiment $I_{th} \approx 5 \times 10^{11}\,\mathrm{W/cm^2}$ [16], with respect to the peak value exceeding $10^{14}\,\mathrm{W/cm^2}$; therefore, the breakdown occurs very early during the laser pulse, and a region of $L_R \approx 100\,\mu\mathrm{m}$ length will be ionized almost instantaneously. After that, the plasma length increases symmetrically (we have an optically thin plasma) up to an extension of $2L_1$. Taking into account I_{th}, the Gaussian increase of the power, the focusing geometry and the velocity of the blast wave typical of our experiment, we estimate $2L_1 \approx 2.8$ mm. The residual expansion of about 150 μm on each side is due to the blast wave, whose mean velocity, considering an expansion time of 5 ns after the pulse peak, would then be 5×10^6 cm/s. We observe that, consistently with the assumption of a radial expansion driven by the cylindrical blast wave, the whole radius of the plasma cylinder is also found to be $\approx 150\,\mu\mathrm{m}$.

The hydrodynamical expansion of a plasma produced by optical breakdown of a gas with a nanosecond laser pulse focused with a large f/N optics appears to be a suitable mechanism to produce waveguides for short pulses. Recently, three possible drawbacks of this method have been underlined [12]. First, for an efficient breakdown, gas density higher than the required densities for LWFA would be required. Second, the energy required would demand a powerful, long pulse, auxiliary laser. Third a significant taper at the waveguide ends has to be expected. This work opens a new route to the possible use of the ASE pre-pulse instead of an auxiliary laser in order to induce the gas breakdown, thus strongly reducing the impact of the first and second drawbacks. As far as the third point is concerned, our measurements indicate that the tapering effect at the channel ends can be drastically reduced if large f/N focusing is adopted, in order to allow the longitudinal expansion to be driven by the propagation of the breakdown threshold condition, rather than by the blast wave.

6 Conclusions

Plasmas produced in a Helium gas-jet have been carefully characterized in their density distribution by the deconvolution, with original algorithms, of high quality interferograms. We found a clear evidence of a regular and reproducible formation of hollow cylindrical channels inside the plasma. The relevant channel parameters were measured, including length, width, electron density at the channel axis and at its boundary. The density at the axis was found to be appropriate for wakefield acceleration driven by pulses of few tens of femtoseconds. Both density jump from the boundary to the axis, and channel width match very well the best guiding condition for focal spots typical of acceleration experiments. The transversal density profile, very close to a parabolic one, allows good propagation of a large number of modes. The channel length of several millimeters can be increased with longer gas-jets and larger f/N numbers. Channels of parameters suitable for a given experiment can be designed using well-established knowledge on the evolution of plasmas produced in gas by optical breakdown. The parameters of the laser pulse we have used are very close to the ones of a typical ASE pedestal of a CPA pulse. This allows one to design experiments in which the ASE is used to preform a channel that is able to guide the femtosecond high power pulse which drives the accelerating plasma waves. This paper represents a new step in the effort of propagating and guiding intense laser pulses in plasmas. Among pioneering works there is early evidence of propagation of a delayed pulse in a pre-formed plasma [27] and the basic study of Ref. [11]. The recent progress includes experiments with clustered gas-jets [12, 13]. Our work is specifically addressed to improve the acceleration capability with ultra-intense laser pulses in plasmas for both self-injected or externally injected electron bunches.

ACKNOWLEDGEMENTS Authors are grateful to the group "Physique Haute Intensité" of CEA-Saclay for having supplied the gas-jet, and in particular to Pascal Monot for many precious information on the gas-jet and data on its characterization. Thanks are also due to the technical staff of IPCF-CNR in Pisa, and in particular to A. Barbini, W. Baldeschi, M. Voliani and A. Rossi. This work, partially supported by the PLASMONX Project of INFN, Italy, was performed in preparation of a series of experiments on laser acceleration to be carried out at the SLIC facility, CEA-Saclay, France, under the European scheme of Access to the Large Facilities, in the framework of the Laserlab Network.

REFERENCES

1 T. Tajima, J.M. Dawson, Phys. Rev. Lett. **43**, 267 (1979)
2 T. Katsouleas, Nature **431**, 515 (2004)
3 S.P.D. Mangles, C.D. Murphy, Z. Najmudin, A.G.R. Thomas, J.L. Collier, A.E. Dangor, E.J. Divall, P.S. Foster, J.G. Gallacher, C.J. Hooker, D.A. Jaroszynski, A.J. Langley, W.B. Mori, P.A. Norreys, F.S. Tsung, R. Viskup, B.R. Walton, K. Krushelnick, Nature **431**, 535 (2004)
4 C.G.R. Geddes, C.S. Toth, J. Van Tilborg, E. Esarey, C.B. Schroeder, D. Bruhwiler, C. Nieter, J. Cary, W.P. Leemans, Nature **431**, 538 (2004)
5 J. Faure, Y. Glinec, A. Pukhov, S. Kiselev, S. Gordienko, E. Lefebvre, J.-P. Rousseau, F. Burgy, V. Malka, Nature **431**, 541 (2004)
6 P. Sprangle, E. Esarey, J. Krall, G. Joyce, Phys. Rev. Lett. **69**, 2200 (1992)
7 W.P. Leemans, C.W. Siders, E. Esarey, N.E. Andreev, G. Shvets, W.B. Mori, IEEE Trans. Plasma Sci. **24**, 331 (1996)
8 E. Esarey, P. Sprangle, J. Krall, A. Ting, IEEE J. of Quantum Electron. QE-33, 1879 (1997)
9 F. Dorchies, J.R. Marquès, B. Cros, G. Matthieussent, C. Courtois, T. Vélikoroussov, P. Audebert, J.P. Geindre, S. Rebibo, G. Hamoniaux, F. Amiranoff, Phys. Rev. Lett. **82**, 4655 (1999)
10 T. Hosokai, M. Kando, H. Dewa, H. Kotaki, S. Kondo, N. Hasegawa, K. Nakajima, K. Horioka, Opt. Lett. **25**, 10 (2000)
11 C.G. Durfee III, H.M. Milchberg, Phys. Rev. Lett. **71**, 2409 (1993)
12 V. Kumarappan, K.Y. Kim, H.M. Milchberg, Phys. Rev. Lett. **94**, 205 004 (2005)

13 H. Sheng, K.Y. Kim, V. Kumarappan, B.D. Layer, H.M. Milchberg, Phys. Rev. E **72**, 036 411 (2005)
14 P. Sprangle, B. Hafizi, J.R. Peñano, R.F. Hubbard, A. Ting, C.I. Moore, D.F. Gordon, A. Zigler, D. Kaganovich, T.M. Antonsen Jr., Phys. Rev. E **63**, 056 405 (2001)
15 D. Giulietti, M. Galimberti, A. Giulietti, L.A. Gizzi, P. Tomassini, M. Borghesi, V. Malka, S. Fritzler, M. Pittman, K. Taphouc, Lett. Phys. Plasmas **9**, 3655 (2002)
16 G.V. Ostrovskaya, A.N. Zaidel', Sov. Phys. Uspekhi **16** (6), 834 (1974)
17 T. Auguste, M. Bougeard, E. Caprin, P. D'Oliveira, P. Monot, Rev. Sci. Instrum. **70**, 2349 (1999)
18 P. Monot, Ph.D. Thesis, Université de Paris-Sud XI, Orsay (1993)
19 R. Benattar, C. Popovics, R. Sigel, Rev. Sci. Instrum. **50**, 1583 (1979)
20 P. Squillacioti, M. Galimberti, L. Labate, P. Tomassini, A. Giulietti, V. Shibkov, F. Zamponi, Phys. Plasmas **11**, 226 (2004)
21 P. Tomassini, A. Giulietti, L.A. Gizzi, M. Galimberti, D. Giulietti, M. Borghesi, O. Willi, Appl. Opt. **40**, 6561 (2001)
22 P. Tomassini, A. Giulietti, Opt. Commun. **199**, 143 (2001)
23 D. Giulietti, A. Giulietti, M. Lucchesi, M. Vaselli, J. Appl. Phys. **58**, 2916 (1985)
24 H.R. Griem, *Principles of PlasmaSpectroscopy* (University Press, Cambridge, 1974)
25 A. Yariv, *Optical Electronics* (Harcourt Brace Jovanovich College Publishers, 1991)
26 C.G. Durfee III, J. Linch, H.M. Milchberg, Opt. Lett. **19**, 23 (1994)
27 A. Giulietti, M. Vaselli, F. Cornolti, D. Giulietti, M. Lucchesi, Rev. Roum. Phys. **32**, 23 (1987)